Modeling the visual pathway for stimulus optimization in brain-computer interfaces

F. Sobreira, C. Tremmel and D.J. Krusienski
Biomedical Engineering
Old Dominion University
Norfolk, VA 23529
Email: fsobr001@odu.edu

***Abstract*—Common brain-computer interface (BCI) paradigms such as P300 Speller and steady-state visual evoked potential (SSVEP)-based interfaces use brain responses to visual stimuli to identify the user's intended target to achieve device control. Many BCI paradigms and decoding approaches do not directly consider the underlying physiology of the sensory pathway and brain responses. By accurately modeling the sensory pathway, it is possible to design new spatial and temporal stimulus patterns to enhance brain response characteristics. This study presents a combined model of the human retina with an artificial neural network (ANN) in order to estimate electroencephalographic (EEG) brain activity trained on actual EEG data. Based on this new visual pathway model, techniques can be developed to create and validate improved stimulus sequences for BCIs and other neurotechnologies.**

I. Introduction

Brain-computer interface (BCI) research has matured over several decades and has produced schemes that are approaching practical information transfer rates (ITRs). The ITRs of current high-speed spelling techniques based on non-invasive BCIs are on the order of ~ 0.8 bit/s for P300 [1] and ~ 4.5 bit/s for steady-state visual evoked potentials (SSVEP) [2]. Advances have been made in the interface design [3], stimulus design [4], and classification schemes [5] for these paradigms. In particular, studies have shown that the spatial and temporal patterns of the visual stimuli can significantly impact the EEG responses and, hence, BCI performance. Waytowich et al. showed that a specific spatial frequency of an SSVEP checkerboard achieves a desirable balance in BCI performance and user preference measured by visual irritation [4]. Bin et al. showed that it is possible to eliminate frequency biases prevalent in fixed-frequency SSVEP paradigms by instead using temporal flashing codes such as pseudorandom sequences [6].

While it is clearly evident that the spatial and temporal characteristics of the visual stimulus will impact the resulting EEG responses, the aforementioned studies derived and tested the stimulus parameters empirically with little or no basis on physiology. In order to further optimize visual stimuli design for enhancing EEG responses, the electrophysiology of the visual pathway to the cortex, and scalp for surface EEG, should be considered. Components of this pathway have been previously modeled including the human retina [7],[8], the generation of VEPs [9], the primary visual cortex (V1) [10], cortical neurons [11], and modeling EEG from cortical neurons [12]. Most of these models are designed as stand-alone components and have not been implemented in combination with other models to represent the full visual pathway to the brain. Additionally, some parts of the pathway, particularly between the retina and V1, including the lateral geniculate nucleus (LGN), do not have well-established models.

The proposed model represents a preliminary approach to reproduce EEG measured over the visual cortex using incoming light intensity as the input to the model. This model combines existing work on the virtual retina [7] with a feedforward artificial neural network (ANN) that will be trained using actual EEG data to match the function of the pathway between retina and an EEG electrode. Future work will further refine this preliminary coarse model of the visual-to-EEG pathway with more sophisticated and physiologically-inspired models, particularly of the retina-V1 pathway. The ultimate objective of this effort is use the model to design optimal spatio-temporal visual stimulus sequences that maximize and/or maximally discriminate some relevant measure of EEG to enhance detection and performance in BCIs and other neurotechnologies. It is envisioned that the proposed models can be extended to optimize stimuli for other physiological responses and sensory pathways.

II. Methodology

The basic visual pathway model consists of a virtual retina model followed by a feedforward ANN as an initial, non-specific model of the retina to cortex pathway, as illustrated in Figure 1. Binary image sequences were presented to a virtual retina model that performs a series of spatio-temporal linear filtering that represent the different layers in the human retina. The resulting voltage at the ganglion cells is then transformed into simulated action potentials that are subsequently applied to the ANN. The ANN is trained using actual EEG to simulate a visual-evoked potential (VEP) from a single or multiple channels over the visual cortex (i.e., Oz).

A. Virtual Retina Model

The virtual retina model describes conversion of a light stimulus incident on the human retina to an electrical stimulus at the visual nerve in 3 stages. The first stage, the outer plexiform layer, represents photoreceptor and horizontal cells

ISBN 978-90-827970-1-5

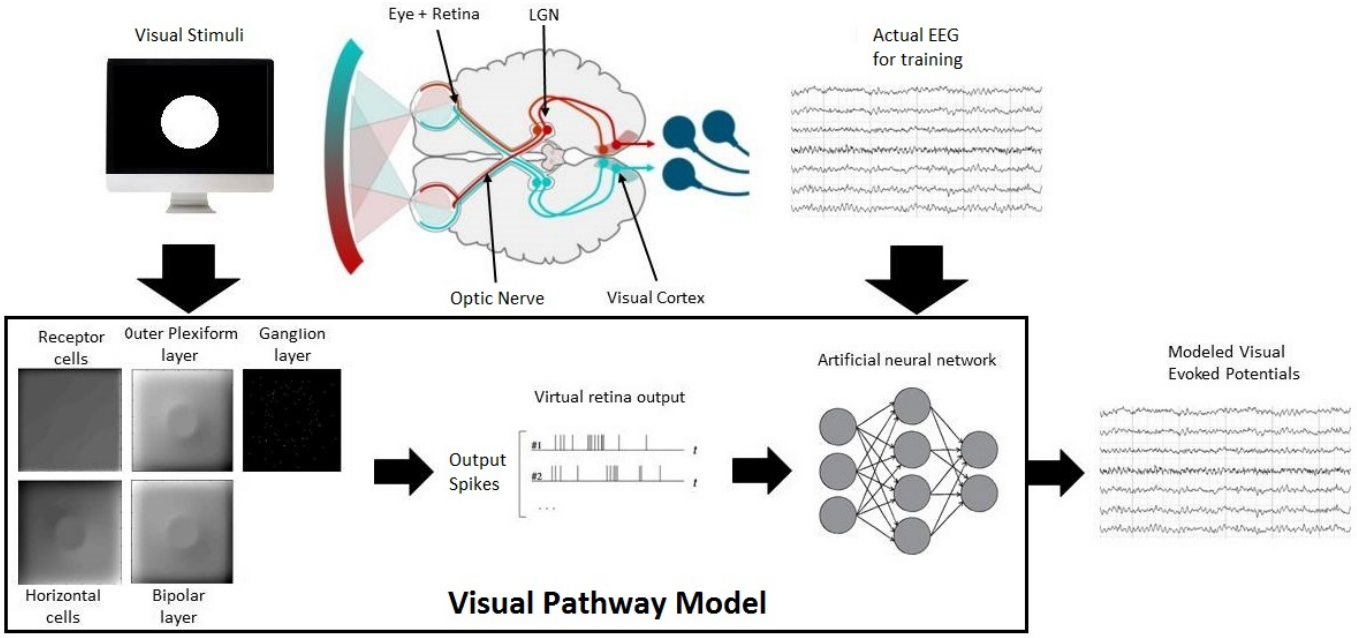

Fig. 1. A block diagram of the model. Flashed binary images were presented to the subject and used as input to the visual pathway model. The actual EEG was used to train an artificial neural network to replicate the VEPs.

and is modeled as a spatio-temporal Gaussian filter. The second stage, the inner plaxiform layer, represents bipolar and amacrine cells and achieves contrast gain control through a nonlinear feedback loop. The last stage, the ganglion layer, adds another spatio-temporal filter to the IPL output and generates action potentials in the ganglion cells using a noisy integral-and-fire neuron model.

The virtual retina was parametrized to simulate a human retina with contrast gain control and one output ganglion layer. A temporal step of $0.01ms$ was set for the calculation, and an input luminosity range from 0 to 255 using a resolution of 50 pixels per retina degree (roughly simulating a screen perception located $50cm$ from the eye). This configuration provides 400 spiking cells output, organized in a square configuration of 20 X 20 cells.

B. Visual Stimuli

The image sequences presented to the virtual retina model were presented for $200ms$ with $600ms$ of empty (black) screen before and after each image presentation. Ten different target images were designed for this experiment, sized 640×640 pixels on a black background. Four images are basic geometric designs (two squares with edges of 200 and 400 pixels, respectively; two circles with diameter of 200 pixels and 400 pixels, respectively), three spirals with widths of 20, 40 and 80, respectively; and three checkerboards with spatial frequency of 0.15, 0.3 and 2.4 cycles/deg, respectively. Figure 3 depicts each respective target image.

There are several motives for selecting the various target images. The virtual retina model contains a contrast detection mechanism that produces more action potentials for more contrast edges in the image. Hence, the spirals and the checkerboards were included. Additionally, for similar reasons, checkerboard patterns are also commonly used as SSVEP-BCI stimuli. Based on Waytowich et. al. [4], the three spatial frequencies that generate the highest classification rates were selected. The squares and circles were selected as a more general representation of the type of stimuli used for the P300 speller.

C. EEG Data Collection and Processing

Data were collected from two able-bodied subjects seated in a comfortable chair, 50 cm from a $21''$ monitor in a dark room. The ten targets were presented to each subject. Similar to the virtual retina model, stimuli were presented $200ms$ and with $3000ms$ inter-stimulus interval to prevent noise of previous target. Signals were sampled at $256Hz$ using an EEG amplifier with 16 active-wet electrodes (g.USBamp, g.GAMMAsys, g.tec, Austria) and were bandpass-filtered between 1 and 60 Hz. A $60Hz$ notch filter was applied to reduce power-line interference. The locations of the 16 EEG electrodes (10-20 system) are shown in Figure 3: Oz, PO7, PO8, P4, P3, Pz, Cz, Fz, PO4, PO3, P6, P5, CPz, C4, C3, ground at FPz, and reference at the left earlobe.

Each subject completed 2 blocks of 18 to 20 runs of the 10 targets images, with the image order presented in a block-randomized fashion. The VEP windows were extracted from $600ms$ prior to the stimulus to $800ms$ post-stimulus. The VEPs were smoothed using a bandpass of $1 - 10Hz$ and downsampled by factor of 4, generating 90 output samples per channel. Only the 8 channels over the visual cortex were used for analysis: Oz, PO7, PO8, P4, P3, Pz, PO4, and PO3.

ISBN 978-90-827970-1-5 © EURASIP 2018

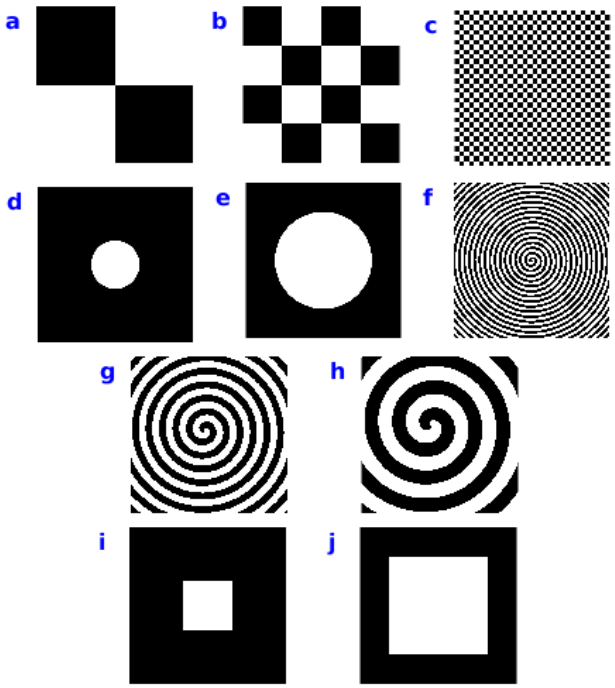

Fig. 2. Target images, a) Checkerboard $0.15c/deg$, b) Checkerboard $0.3c/deg$, c) Checkerboard $2.4c/deg$, d) Circle $d = 200$ pixels, e) Circle $d = 400$ pixels, f) Spiral $w = 20$ pixels, g) Spiral $w = 40$ pixels, h) Spiral $w = 80$ pixels, i) Square $l = 200$ pixels and j) Square $l = 400$ pixels

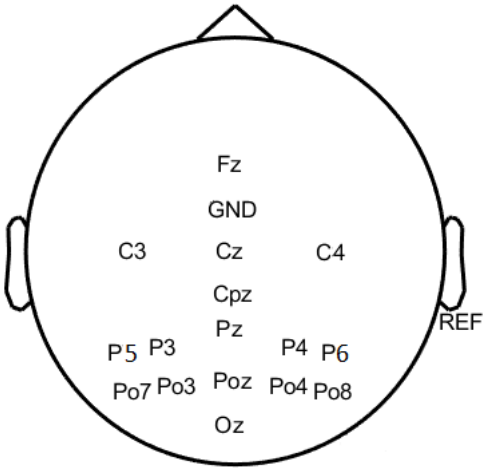

Fig. 3. Electrode montage used for this study.

D. Retina-EEG Modeling

A feedforward Artificial Neural Network (ANN) was used to process the simulated action potentials (spikes) and estimate the VEP for each stimulus input. The ANN was composed of three hidden layers with 200 hidden units each and train on the actual VEPs. At the output of the virtual retina, the spikes were spatially rescaled to 50% of the original size using a bicubic interpolation method and the frames were downsampled by factor of 5, resulting in 1700 features for each image target that were used as input for the ANN. To roughly model the noise in the VEP response due to the fact that no signal-trial VEPs to a given image stimulus will be identical, Gaussian white noise at $\pm 2.5\%$ of the single-trial amplitude range was added to the data [13].

The data from both subjects combined were used to train the ANN. The data were divided into 80% of the trials for training and the remaining 20% as an independent test set. The training data was further subdivided into 70%, 15%, and 15% respectively for training, validation, and testing. For increased computational efficiency, the scaled conjugate gradient function was used to train the ANN with parallel working GPU cores, and 5-fold cross validation was performed.

III. Results

The visual pathway model was able to reproduce simulated VEPs that are highly correlated with the actual VEPs and also are discriminable across the various input images. Figure 4 shows a comparison of the simulated and actual VEP waveforms, averaged across the 8 visual cortex electrodes, for a given target image. While the salient amplitude peaks are clearly aligned, the simulated VEP is slightly attenuated.

The Pearson correlation coefficient was computed between each pair of simulated and actual VEP waveforms, averaged across the 8 visual cortex electrodes. To simplify the comparisons and evaluate the equivalent of a 4-class BCI, the results from 4 images that produced the largest differences in average correlations within and across the target images (images b, c, i, and j from Figure 2).

Figure 5 shows the Pearson correlation coefficients between the actual VEPs across the subset of 4 target images. In comparison, Figure 6 shows that for the same image subset, the simulated an actual VEP waveforms are highly correlated (median correlation 0.91) for the same target image, while the correlations are significantly reduced when comparing between different target images (median correlation 0.48). Thus, the model preserves the subtle differences and discriminability of the actual VEPs for different target images.

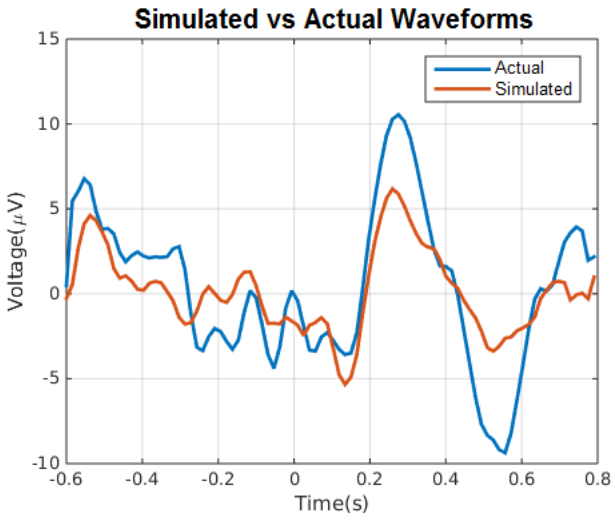

Fig. 4. Example waveforms for simulated and actual VEPs averaged across the 8 visual cortex electrodes.

ISBN 978-90-827970-1-5 © EURASIP 2018

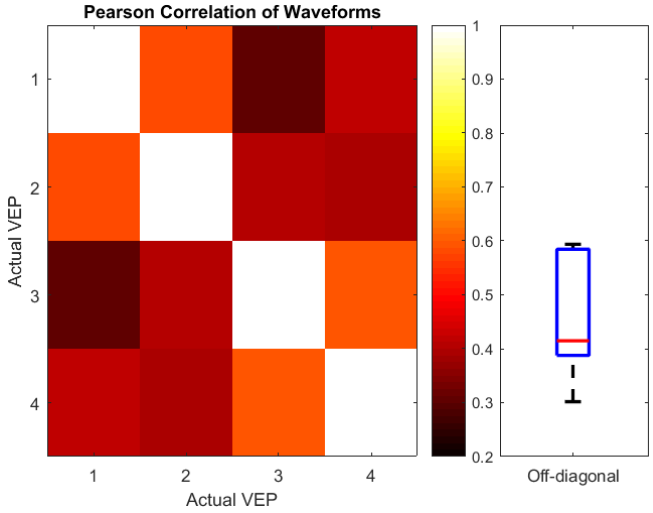

Fig. 5. (Left) Correlation between actual VEP waveforms for 4 different target images. (Right) Correlation box plot the non-intended targets (off-diagonal). The correlation is 1 for the diagonal elements.

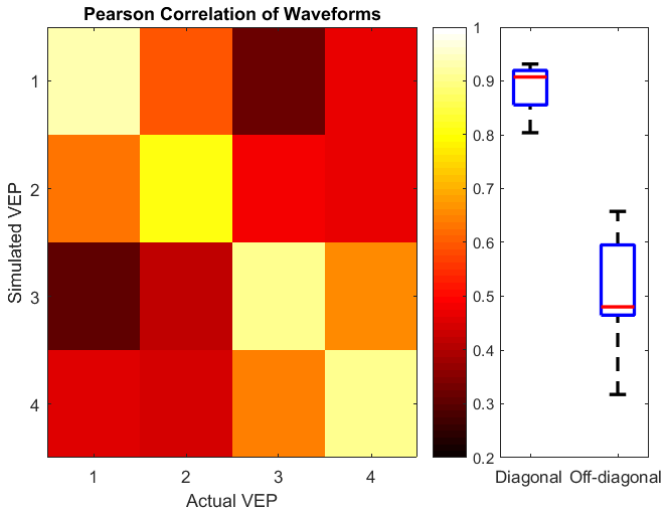

Fig. 6. (Left) Correlation between actual and simulated VEP waveforms for 4 target images. (Right) Correlation box plot for the intended targets (diagonal) and non-intended targets (off-diagonal).

IV. Discussion

The proposed visual pathway model, extending the virtual retina with an Artificial Neural Network, proved to be effective for simulating distinct VEPs from different binary target images. The correlations between the actual and simulated VEPs for the same target image reached 0.93 with a median of 0.91, while the median correlation between different target images was 0.48. This demonstrates that the model has highly consistent performance in simulating the desired VEP across different target images while remaining distinct from the VEPs from other target images. Further analysis is needed to understand exactly how the spatial patterns of the images affect the simulated EEG based on the model. More systematic image patterns will be developed and tested, considering important parameters for comparisons such as fixing the average contrast of the input images and local spatial features.

Using such models, the spatio-temporal parameters of the visual stimulus patterns that maximize and/or maximally discriminate some relevant measure of EEG can be determined empirically, analytically, or computationally. Future work will aim to make the model more biologically plausible and amenable for tractable optimization using information theoretic techniques, for instance. An example of a biologically plausible approach is to replace the ANN with a three-dimensional neuronal network to model the various layers of the visual cortex. In this approach, the training algorithm would not train the strength of the connections of the different layers but actually form connections between the neurons as in biological neural networks [11]. Additionally, the resulting neurons could be modeled as electric dipoles for estimation of the scalp potentials through inverse modeling.

Using this approach, subject-specific or subject-independent models can be created and the physiologically-optimal stimuli can be designed to enhance the performance of BCIs and other neurotechnologies. Furthermore, the modeling and optimization framework can be adapted for any sensory pathway to the brain, and potentially any physiological output signal.

Acknowledgment

Research supported in part by the National Science Foundation (1421948).

References

[1] H. Sato and Y. Washizawa, "An N100-P300 Spelling Brain-Computer Interface with Detection of Intentional Control." in Computers 5(4), 2016, 31.

[2] X. Chen et al., "High-speed spelling with a noninvasive braincomputer interface." in Proceedings of the national academy of sciences 112(44), 2015: E6058-E6067.

[3] N. Waytowich and D. J. Krusienski, "Spatial decoupling of targets and flashing stimuli for visual braincomputer interfaces," in Journal of Neural Engineering, 12, 2015.

[4] N. Waytowich, Y. Yamani, and D. J. Krusienski. "Optimization of Checkerboard Spatial Frequencies for Steady-State Visual Evoked Potential Brain-Computer Interfaces." in IEEE Transactions on Neural Systems and Rehabilitation Engineering, 2016.

[5] H. Wang et al., "Discriminative Feature Extraction via Multivariate Linear Regression for SSVEP-based BCI" in IEEE Trans. on Neural Systems and Rehabilitation Engineering, 24(5), 2016, 532-41.

[6] G. Bin et al. "A high-speed BCI based on code modulation VEP." in Journal of Neural Engineering 8, 2011, 025015.

[7] A. Wohrer and P. Kornprobst, "Virtual retina: a biological retina model and simulator, with contrast gain control." in Journal of computational neuroscience, 26.2, 2009, 219-249.

[8] S. Tlu, "Mathematical models of human retina." in Oftalmologia, 55(3), Bucharest, Romania, 2010, 74-81.

[9] B. H. Jansen and V. G. Rit, "Electroencephalogram and visual evoked potential generation in a mathematical model of coupled cortical columns." in Biological cybernetics 73(4), 1995, 357-366.

[10] D. McLaughlin, R. Shapley and M. Shelley, "Large-scale modeling of the primary visual cortex: influence of cortical architecture upon neuronal response." in Journal of Physiology-Paris 97(2), 2003, 237-252.

[11] E.M. Izhikevich, "Simple model of spiking neurons." in IEEE Transactions on neural networks, 14(6), 2003, 1569-1572.

[12] R. Grech et al., "Review on solving the inverse problem in EEG source analysis." in Journal of neuroengineering and rehabilitation, 5(1), 2008, 25.

[13] H. Jianping et al., "Noise-injected neural networks show promise for use on small-sample expression data." in BMC Bioinformatics, 2006, 7:274.

ISBN 978-90-827970-1-5 © EURASIP 2018